Synthesis and characterization of several rhenium(I) complexes of 2-acetylpyridine and ferrocenyl carbaldehyde derivatives of 2-hydroxybenzoic acid hydrazide

Paula Barbazán,[a] Rosa Carballo,[a] Inmaculada Prieto,[b] Margarita Turnes,[b] Ezequiel M. Vázquez-López.[a,*]

[a]Departamento de Química Inorgánica, Facultade de Química, Universidade de Vigo, E-36310 Vigo, Galicia – Spain.

[b]Departamento de Química Física, Facultade de Química, Universidade de Vigo, E-36310 Vigo, Galicia – Spain.

Abstract.- The rhenium(I) carbonyl halide (X = Cl and Br) complexes, $[ReX(CO)_3\{H_2(py)L^2\}]$ (**1a**, **1b**) and $[ReX(CO)_3\{H_2(Fc)L^2\}]$ (**2a**, **2b**), of the ligands derived from 2-acetylpyridine and ferrocenyl carbaldehyde derivatives of 2-hydroxybenzoic acid hydrazide [$H_2(py)L^2$ and $H_2(Fc)L^2$, respectively] have been prepared in good yield. The complexes have been characterized by elemental analysis, MS, IR, UV-vis and ^{1}H NMR spectroscopic methods and their structures have been elucidated by X-ray diffraction. The ligand forms a five-membered chelate ring but in $H_2(py)L^2$ it is $N_{pyridine}$,N'-bidentate while it is O,N-bidentate in $H_2(Fc)L^2$ complexes. Reaction of complex **1a** with copper(II) nitrate yields the unexpected aqua complex $[Re\{H(py)L^2\}(H_2O)(CO)_3]$ (**3**) where the ligand is monodeprotonated but maintains the coordination mode observed in **1a**, as shown by X-ray diffraction. However, reaction of

* Corresponding author: Tel.: +34 986 812319; fax: +34 986 812556 (E.M. Vázquez-López).
E-mail address: ezequiel@uvigo.es (E.M. Vázquez-López).

1b with glycine yields a conformational polymorph of the original compound, **1b'**. The X-ray study shows that the orientation of the O–H phenol group against the carbonyl amide group is the main difference.

1. Introduction

There is growing interest in carbonyl rhenium(I) complexes with 2-pyridine aldehyde and 2-acetylpyridine derivatives as a way to conjugate the $\{M(CO)_3\}^+$ (M = ^{188}Re and ^{99m}Tc) fragment for the labelling of targeting biomolecules. Alberto *et al*. showed that the ketone or aldehyde is activated by coordination to the *fac*-$[Re(CO)_3]^+$ moiety and that the reaction with several (bio)molecules containing primary amines yields the corresponding N,N'-diimine complexes, with rates of formation several orders of magnitude faster than the reaction between free aldehyde, ketone and amine [1]. This strategy has also been employed to obtain Lipidiol surrogates as possible agents for liver cancer imaging and therapy [2] or to introduce amino acids or esters [3,4]. In addition to labelling properties, the introduction of binding groups such as aza-crown has been carried out in order to assay their properties in cation and molecular recognition studies (see for example ref. [5]). Furthermore, the luminescent properties of rhenium(I) tricarbonyl N,N'-diimine complexes have demonstrated to have applications in biological imaging as fluorochromes in fluorescence microscopy [6a]. The large Stokes shifts, long lifetimes and good quantum yields allow easy differentiation of their emission from interfering autofluorescence [6b].

Hydrazine derivatives containing N-heterocycles and their complexes exhibit strong antitumor and antivirus activities [7]. The antimicrobial activities of copper complexes of these compounds have also been reported [8]. As a consequence, the 2-acetylpyridine derivatives of these systems are an interesting group of candidates to design molecules for labelling. In contrast, we did not find any evidence that the reaction of 2-acetylpyridine coordinated to rhenium(I) yielded the corresponding hydrazone complexes by reaction with salicylaldehyde hydrazide [9], but the synthesis of the same target complex from the previously isolated ligand is straightforward. As a result, several rhenium(I) acetylpyridine hydrazones have recently been reported [10-12].

Recently, rhenium(I) complexes of 2-acetylpyridine benzoylhydrazone [10] [H(py)L^1 in Scheme 1] have been synthesized. The ferrocenyl analog, H(Fc)L^1 in Scheme 1, was also prepared because of the potentially improved antitumor and antivirus activities of the ferrocenyl group [13, 14] and the possibility of modulating the binding affinity of the ligand for the rhenium fragment by altering the redox state [15]. These studies show that the differences in the coordination of the ligand; κ-*N,N′* in H(py)L^1 and κ-*N,O* in H(Fc)L^1, cause different spectroscopic behavior (mainly in ^{1}H NMR spectroscopy).

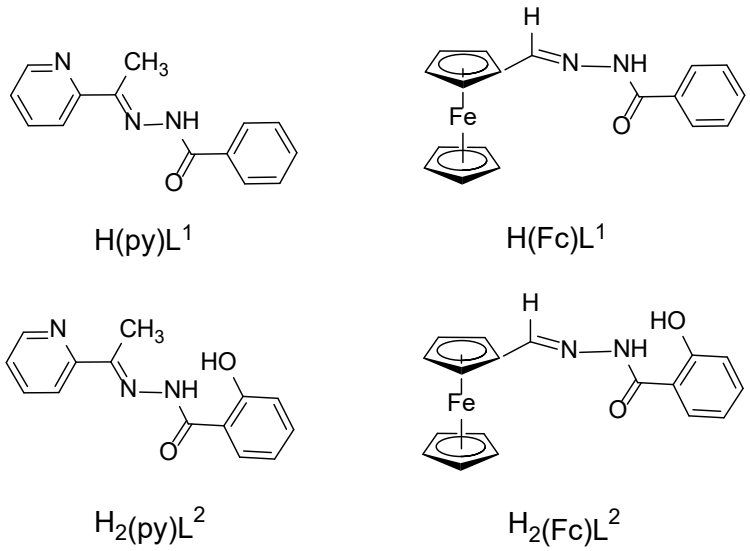

Scheme 1

In the present paper, we report a study of hydrazones derived from 2-hydroxybenzoic acid and 2-acetylpyridine and ferrocenyl carbaldehyde [H_2(py)L^2 and H_2(Fc)L^2 in Scheme 1, respectively]. Both compounds are potentially diprotic ligands and they may act as tetra- or tridentate planar chelating agents that coordinate through the phenolic hydroxy, amide oxygen and one/two imine nitrogen atoms. However, in the copper(II) and zinc(II) complexes of the pyridine derivatives reported, we observed exclusively the tridentate monodeprotonated ligand $[H(py)L^2]^-$ [16]. The structural data for H_2(Fc)L^2 are even more scarce, although the presence of a bidentate neutral ligand has been reported in a ruthenium(II) complex [17].

2. Results and Discussion

2.1 Synthesis and spectroscopic characterization

Reactions of the ligands $H_2(py)L^2$ and $H_2(Fc)L^2$ with the adducts *fac*-$[ReX(CO)_3(CH_3CN)_2]$ afforded orange or red solids that are stable in air, moderately soluble in organic solvents – such as toluene, chloroform and ethanol – and highly soluble in acetone. Elemental analysis and mass spectrometry confirmed the stoichiometries $[ReX(CO)_3\{H_2(py)L^2\}]$ (**1**) and $[ReX(CO)_3\{H_2(Fc)L^2\}]$ (**2**) (Scheme 2).

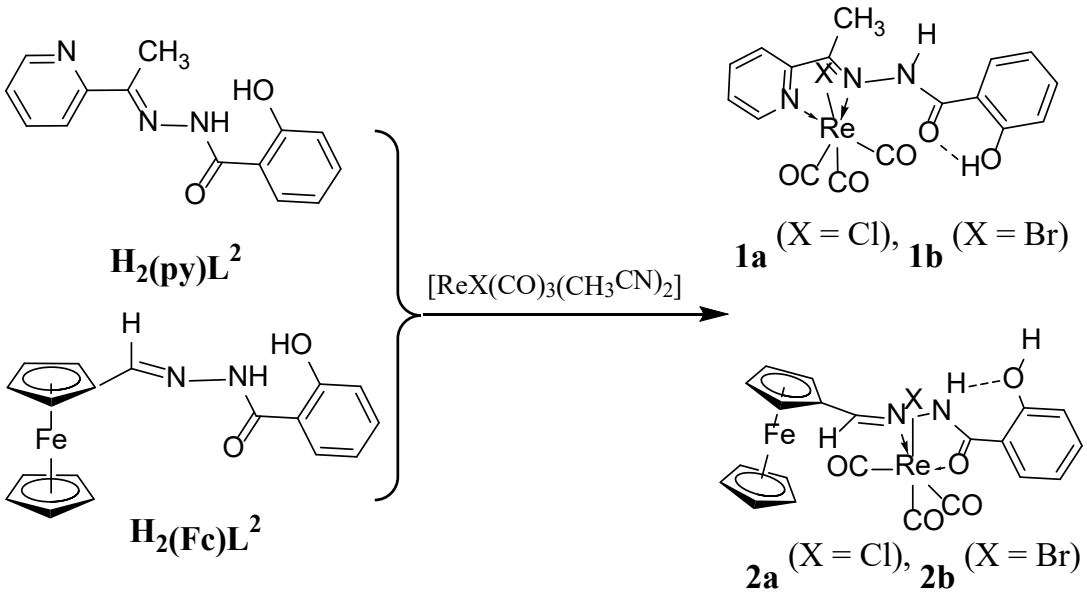

Scheme 2

The mass spectra contain the signal corresponding to the molecular ion although the peaks due to the species $[M - X]^+$ are more intense, as observed in the rhenium(I) complexes of benzoylhydrazones [9, 15] and thiosemicarbazone derivatives [18]. A facial geometry around the rhenium atom is suggested by the three strong ν(C≡O) IR bands in the range 2027–1892 cm^{-1} in the complexes.

The solutions of ferrocene derivatives show evidence of decomposition when stored for days in sunlight. We have tested the formation of heterodinuclear complexes and co-crystals by reaction of the rhenium derivatives with metallic acetates [zinc(II) or copper(II)], aromatic amines or amino acids, unsuccessfully. In fact, diffusion

experiment of an acetone solution of **2a** into a MeOH solution of copper(II) acetate afforded few single crystals of the metallocrown complex $[Fe_{10}(O_2CCH_3)_{10}(OCH_3)_{20}]$, as determined by X-ray diffraction [19]. However, the presence of metal nitrates in aqueous solutions of $H_2(py)L^2$ derivatives yielded some single crystals of $[Re\{H(py)L^2\}(H_2O)(CO)_3]$ (**3**).

2.2 X-ray studies

*2.2.1 The crystal and molecular structure of the 2-acetylpyridine-salicyloylhydrazone adducts $[ReX(CO)_3\{H_2(py)L^2\}]$ (**1a**, **1b** and **1b'**)*

The complexes $[ReX(CO)_3\{H_2(py)L^2\}]$ (**1a**, **1b**) are isotypic and crystallize in the monoclinic $P2_1/n$ space group. The molecular structures of the complexes are shown in Figures 1A and 1B along with the atomic numbering scheme used. Selected bond lengths and angles for both complexes are listed in Table 1.

The rhenium atom is coordinated by the N(2) hydrazone and N(3) pyridine atoms, affording a five-membered chelate ring, as well as three carbonyl carbon atoms and a halide atom. The resulting coordination geometry can be described as distorted octahedral [the main distortion being the N(2)–Re–N(3) and C(22)–Re–N(2) angles]. The differences between these angles are statistically insignificant apart from the expected longer Re–Br distance than Re–Cl and the N(2)=C(8) distance in **1a** being clearly shorter than in **1b**. The latter distance in **1a** is statistically equivalent to that observed in the free ligand [1.285(4) Å] [16] and in its hydrochloride form [1.288(2) Å] [20] while that in **1b** is similar to that found in the ferrocene derivatives **2** (vide infra).

Other interesting differences with respect to the free ligand structure are the change in the orientation of the pyridine nitrogen atom to allow N,N' coordination to the rhenium and the loss of the planarity observed in the free form [16] by rotation around the N(1)–

N(2) bond. Consequently, the angle between the planes defined by the salicylaldehyde and pyridine groups (see Scheme 3) is greater than 60º.

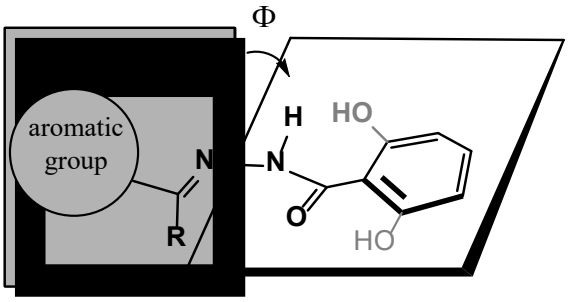

Comp.		R	Φ(º)
1a	py	Me	62.6
1b	py	Me	64.7
1b'	py	Me	45.1, 50.7
2a	Fc	H	13.6
2b	Fc	H	22.1
3	py	Me	48.3

Scheme 3

There is also rotation around the C(1)–C(2) bond, meaning that the intramolecular hydrogen bond N(1)–H…O(2) observed in the free ligand is broken and replaced by the interaction O(2)–H…O(1). The distances between donor-acceptor atoms in both interactions, i.e. the distances N(1)–O(2) in $H_2(py)L^2$ and $[H_3(py)L^2]^+$ and O(2)–O(1) in complexes **1a,b**, are very similar (see Table 2).

The molecules are associated into dimers by a weak hydrogen bond N(1)–H…X^i (see Table 2 and Figure 2A). We observed a similar association in other rhenium(I) halide complexes with hydrazone and thiosemicarbazone ligands [15, 18, 21]. These dimers are packed through weak C–H…$O_{carbonyl}$ hydrogen bonds.

In addition, few single orange crystals obtained by diffusion of an acetone/water glycine solution to an acetone solution of *fac*-$[ReBr(CO)_3\{H_2(py)L^2\}]$ shows different cell parameters compared to those described above (**1b'**). X-ray analysis of these crystals showed two independent molecules per asymmetric unit and, furthermore, non-merohedral twinning (two components were identified). In any case, the structure was solved and proved to be a conformational polymorph (Figure 1C) of the arrangement found previously. The main differences are the orientation of the hydroxyl group and its role (acceptor/donor) in the intramolecular hydrogen bond. In **1b'** the orientations of the

carbonyl amide and hydroxyl groups diverge in such a way that the N–H group establishes an interaction with the –OH in a similar way to that observed in the free ligand. However, this interaction is unable to impose a planar conformation on the ligand and the N…O distance is slightly lengthened.

On the other hand, apart from the Re–N(2) distance, which is slightly shorter in **1b'** than in **1b**, the bond distances and angles are statistically equivalent in both forms.

The free N–H groups in **1a** and **1b** are too sterically hindered to play a relevant role in the crystal packing (as depicted in the Figure 1B), but in **1b'** the –OH group establishes moderate interactions as a donor with the oxygen carbonyl group of neighboring molecules. This interaction seems mandatory in the crystal packing but it is also supported by weaker interactions between the N–H group and the metal carbonyl groups (Figure 2B). In this way both interactions contribute to the association of the molecules in chains running along the *b* axis.

*2.2.2 The crystal and molecular structure of the ferrocenylcarbaldehyde-salicyloylhydrazone adducts [ReCl(CO)$_3${H$_2$(Fc)L^2}].H$_2$O (**2a**) and [ReBr(CO)$_3${H$_2$(Fc)L^2}].(EtOH) (**2b**)*

The molecular structures of the ferrocenylaldehyde derivatives are depicted in Figures 3A and 3B. Unfortunately, we were unable to obtain suitable single crystals of the ligand H$_2$(Fc)L^2 for comparison with these structures. Compounds **2a** and **2b** were isolated as water and ethanol solvates, respectively. The rhenium atom is coordinated in both structures by the N(2) and O(1) hydrazone atoms to give a five-membered chelate ring, as well as by three carbonyl carbon atoms and the halogen atom. The Re–O(1) and Re–N(2) distances are similar to those observed in the complex [ReBr(CO)$_3${H(Fc)L^1}] [15] although some differences can be highlighted concerning the conformation of the ligand. Firstly, in the present structures the configuration around the C(8)=N(2) bond is

Z, meaning that the H atom is directed towards the fragment $\{Re(CO)_3\}^+$. The conformation around this bond in the structure of $[ReBr(CO)_3\{H(Fc)L^1\}]$ [15] is E. In the latter complex the metal-ligand link seems to be flexible enough to avoid the steric hindrance imposed by the ferrocenyl group, giving rise to a non-planar chelate ring. In the present case, however, the absence of this hindrance means that the rhenium atom lies on the hydrazone plane. The energetic difference between the two structures seems be rather low and packing effects can probably overcome the energy gap. In fact, we have observed both conformations in the ferrocenylcarbaldehyde thiosemicarbazones of rhenium(I) adducts and, more surprisingly, a single crystal of each of the conformers of the thiosemicarbazonate complexes was isolated and characterized [18]. Secondly, complexes **2a** and **2b** adopt a different orientation of the halogen with respect to the ferrocenyl group. The chlorine atom in **2a**, as observed in $[ReBr(CO)_3\{H(Fc)L^1\}]$ [15], and the bromine in the thiosemicarbazone adducts of the fragment of $\{ReBr(CO)_3\}$ [18] are oriented towards the opposite side of the ferrocene group (*anti*). However, in **2b** the orientation is towards the same side as the ferrocene group (*syn*). The presence of the two possible orientations in solution was detected by the presence of two sets of ferrocene and hydrazone signals in the ^1H NMR spectra (*vide infra*).

The N,O-coordination of the rhenium in both complexes forces the ligand molecule to establish an intramolecular hydrogen bond, as observed in the structure of free $H_2(py)L^2$ and **1b'**, i.e., once again the N(1)–H group is a donor group while O(2) is a hydrogen bond acceptor. The Φ angle, as defined in Scheme 3, is noticeably lower than in complexes **1a** and **1b** (Scheme 3).

The packing arrangement in both compounds is dominated by the presence of the solvent molecule, which imposes a different situatution to reach a similar molecular association. In both crystals the oxygen solvent atom (water/ethanol) is a hydrogen bond acceptor with the O(2)–H group. In addition, the water molecule, now a hydrogen bond

donor, associates the complex molecules to give centrosymmetric dimers through interaction between one of the hydrogen atoms and the chlorine ligand. The other water hydrogen atom establishes a bifurcated bond with two oxygen carbonyl atoms of two neighboring molecules. These interactions result in the formation of a 2D association, as depicted in Figure 4A. These sheets are parallel to the crystallographic *ab* plane.

In spite of the different crystallographic symmetry, similar association is observed in **2b**. In this case there is a bifurcated donor hydrogen bond with the Br atom of two different neighboring molecules (Figure 4B) and the ethanol is associated with molecules of **2b** in sheets parallel to crystallographic *ab* plane.

*2.2.3 The crystal and molecular structure of the 2-acetylpyridine-salicyloylhydrazonate complex [Re{H(py)L^2}(H$_2$O)(CO)$_3$] (**3**)*

The molecular structure of the complex [Re{H(py)L^2}(H$_2$O)(CO)$_3$] is shown in Figure 5 along with the atomic numbering scheme used. Selected bond lengths and angles are listed in Table 1.

The rhenium atom is coordinated by the N(2) hydrazone and N(3) pyridine atoms, by three carbon carbonyl atoms and by the oxygen atom of a water molecule. The resulting coordination geometry can be described as distorted octahedral [the main distortion being the angle N(2)–Re–N(3)]. The differences in the Re–N distances between the adducts **1a**–**b** and **3** are statistically insignificant. The Re–Ow distance is similar to those found in [Re{(py)L^1}(H$_2$O)(CO)$_3$] [10], the cationic derivatives *mer*,*trans*-[Re(CO)$_3$(H$_2$O)(L)$_2$]$^+$ (2.216–2.263 Å; L = a phosphonite or phosphinite ligand) [22] and the pyrazolonate-aqua complex *fac*-[Re(pyz)(H$_2$O)(CO)$_3$] [2.216(5) and 2.203(6) Å] [21].

The main difference in the ligand bond distances in **3** with respect to the free ligand is that the C(1)–O(1) bond is longer (Table 1). This effect has also been observed in the

complexes [CuBr{H(py)L^2}] and [Zn{H(py)L^2})$_2$] [16]. These findings suggest the predominance of the resonance form shown in Scheme 4 in complex **3**, despite the uncoordinated character of the O(1) atom. As observed in the Zn(II) and Cu(II) complexes, the intramolecular hydrogen bond remains but now the N(1) atom is an acceptor and O(2)–H the donor, with the structural parameters of this bond being very similar in all three compounds (Table 3).

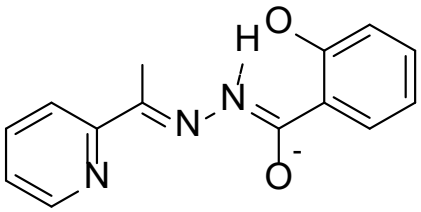

Scheme 4

Furthermore, the O(1) atom is involved in two intra- and intermolecular hydrogen bonds. In the first bond it is an acceptor group for the water molecule coordinated to the rhenium atom. The intermolecular interaction involves the water molecule of a neighboring complex and associates the molecules into centrosymmetric dimers (Figure 5). The metric parameters associated with the two interactions (Table 3) suggest comparable behavior. It is worth noting that, in spite of the intramolecular interaction Ow–H…O(1), the Φ angle (Scheme 3) is lower than in **1a** and **1b**.

These dimers pack through weak C–H…O interactions involving the aromatic C–H group and the metal carbonyl oxygen atoms.

2.3 Solution studies

2.3.1 NMR studies

The ^{1}H NMR spectra of the rhenium(I) complexes and ligands in acetone-d_6 and DMSO-d_6 were acquired and the assignments are included in the experimental section for comparison.

The ^{15}N-HSQC experiments on $H_2(py)L^2$ allowed the assignment of the N–H and O–H signals. The O–H proton is the most deshielded in the spectra (DMSO and acetone) of $H_2(py)L^2$ and the next signal (around 10.70 ppm in acetone and 11.50 ppm in DMSO) is due to the N–H group. The position of the first signal shows a more marked temperature dependence in DMSO-d_6 ($d\delta/dT$ = 8 10^{-3} ppm/deg versus 4 10^{-3} ppm/deg for the N–H group) and this is similar to the effect observed in other rhenium(I) salicylhydrazone complexes [16]. This finding is consistent with the freedom of this O–H group, as shown in the X-ray structures (*vide supra*), changing due to the mobility of the solvent molecules [23].

It was observed that, in general, the C–H proton signals in the rhenium complexes are shifted downfield with respect to those in the free ligand in hydrazone [15] and thiosemicarbazone [18, 21] derivatives. In contrast, the hydrazine proton singlet is strongly shifted (about 2 ppm) when the N–H group is a member of chelate ring, as in $[ReBr(CO)_3\{H(Fc)L^1\}]$, or by around 1 ppm when the N–H group does not form part of the ring, as in $[ReBr(CO)_3\{H(py)L^1\}]$ [15]. The ^{1}H NMR spectra of **1a** and **1b** show substantial deshielding of the proton signals apart from the O–H and N–H groups.

In the search for specific approaches to carry out a coordinative diagnosis of hydrazone and thiosemicarbazone adducts in solution, we were interested in assessing whether this behavior is general.

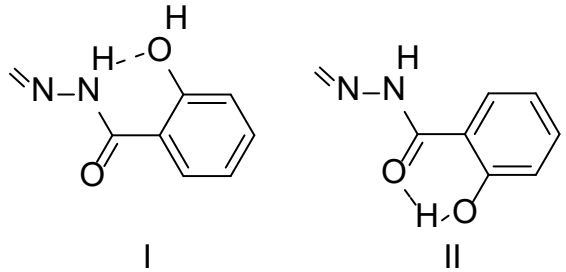

Scheme 5

^{15}N-HSQC experiments were again used to make a reliable assignment of the signals. On coordination, the N(1)–H proton gives rise to the most deshielded signal in the

spectrum (Figure 6) but the signal is only shifted by 1 ppm with respect to that in the free ligand – a finding that is consistent with the N,N'-coordination of the ligand.

In order to assess the utility of the temperature dependence parameter proposed by Leeflang [23], we measured the variation of both signals with temperature in DMSO solutions. It was unusual to find that the dδ/dT parameters for both O–H and N–H signals show low temperature dependence (values between 4.6 and 4.1 10^{-3} ppm/deg,). This finding is consistent with the hydrogen bond O–H…O (structure II in Scheme 5) observed in the solid structure of **1a** and **1b**, although one should expect a larger dδ/dT for the signal of the newly released N(1)–H group. Two factors may explain these discrepancies: (i) steric factors disfavor substantially the hydrogen bond donor character of the N(1)–H group (as emphasized in Figure 1B and shown by the poor role of this group in the molecular association, see Table 2). In fact, the insensitivity to hydrogen bonding of several secondary amides in DMSO solution and the solid state has been reported by McQuade *et al.* [24] and this was also attributed to steric hindrance. (ii) The presence of conformation I (Scheme 5) that observed in the solid of polymorph **1b'**, may affect the positions of the signals in DMSO solution. Although we obtained several crystals under different conditions, the corresponding study showed the presence of polymorphic forms of **1a** and **1b** in all cases. In fact, **1b'** seems to be a kinetic product obtained in a diffusion experiment. Thus, we believe that the latter explanation is unlikely. In any case, these results invalidate the temperature dependence studies to determine the nature of the group involved in the intramolecular hydrogen bonding in these compounds.

The NMR studies of the ferrocene derivative, $H_2(Fc)L^2$, and its complexes **2a** and **2b** were restricted by the lack of stability of the rhenium complexes in DMSO. As a result, the dδ/dT values for both complexes were not determined.

The assignment of the N–H and O–H signals in the free ligand is based on the ^{15}N-HSQC experiments at similar positions to the pyridine compound. The lack of stability of **2a** and **2b** also preclude the use of these studies and therefore the assignment of the N–H and O–H proton signals is based on the position in the [ReX(CO)$_3${H(Fc)L^1}] complexes and assumes a strong deshielding of the N(1)–H signal after the formation of the chelate ring by N,O-coordination of the ligand.

2.3.2 UV-vis spectra

The UV-vis solution spectra of the ligands H$_2$(py)L^2 and H$_2$(Fc)L^2 and their complexes were recorded and the main data are included in Table 3.

The spectra of the ferrocene derivatives are strongly dominated by the ferrocene bands, which have been discussed by Sohn *et al*. [25]. The spectra of the compounds were obtained in two solvents of different polarity, such as methanol and chloroform, and suggest a slight positive hyperchromic effect – except for H$_2$(Fc)L^2.

Firstly, the spectra of the free ligand will be discussed. The absorptions in the range 300–360 nm and bands centered at 260 nm in the ferrocene derivatives are due to π-π^* transitions, the latter probably those of cyclopentadienyl rings [17]. The band centered at 300 nm, which is present in the uncoordinated ligands, is attributed to the IL π-π^* transitions, probably from the aroylhydrazone moiety [17], and this hardly changes upon coordination to rhenium. The shoulder between 430–460 nm in the H$_2$(Fc)L^2 derivatives is attributed to MLCT from iron to cyclopentadienyl rings. Finally, the bands near to 420 nm in **1a** and **1b** and 500 nm in **2a** and **2b** are assigned to MLCT transitions from the rhenium to the hydrazone ligand [26a].

As observed in other hydrazone complexes based 2-acethylpyridine [9], the emission of **1a** and **1b** is negligible at room temperature. The strong red shift of the MLTC bands

(absorption and emission) in hydrazone complexes when compares with N,N'-diimine analogs explains the different photophysics properties [26b].

2.3.3 Electrochemistry studies

Cyclic voltammetry results for the ligand $H_2(Fc)L^2$ and its complexes **2a** and **2b** in the range –0.4 to 1.3 V in CH_2Cl_2 are listed in Table 3. The voltammograms show the typical form for a process dominated by diffusion and this is attributable to the monoelectronic oxidation of the ferrocenyl group. The separation between waves corresponding to the anodic and cathodic process is similar to that shown by ferrocene itself under the same experimental conditions. Thus, the electrochemical behavior is a typical quasi-reversible process.

The cyclic voltammetric response of $H_2(Fe)L^2$ (0.554 V in CH_2Cl_2) is shifted with respect to that in free ferrocene (0.450 V) and suggests electronic withdrawing character of the hydrazone arm over the ferrocenyl group, thus making the oxidation more difficult. A similar process was observed by Graudo *et al.* in semicarbazone and thiosemicarbazone derivatives of ferrocene [27].

On the other hand, the N,O-coordination makes the oxidation of the ferrocene group more difficult, a finding in agreement with a higher acceptor character on the active group – as concluded from the $E_{1/2}$ value obtained for **2a** and **2b** (0.730 and 0.720 V, respectively). These values are higher than that observed for $[Ru(bpy)_2\{H_2(Fc)L^2\}]$ in acetonitrile (0.60 V) [17], suggesting a higher electronic acceptor character for the fragment $\{Re(CO)_3\}^+$ in comparison to $\{Ru(bpy)_2\}^{2+}$ in spite of the different formal charge.

3. Conclusions

The present results, along with those from earlier studies [15, 16, 18, 21], indicate that NMR spectroscopy can be used to determine the coordination behavior of hydrazones in solution on the basis of the chemical shift of the N(1)–H proton. However, the use of parameters such as the temperature dependence of this signal to evaluate the role of the groups in intramolecular hydrogen bonding is ruled out.

The derivatives of $H_2(Fc)L^2$, in which the ligand acts in an O,N-bidentate manner, have lower stability than the other complexes. Work is in progress to determine the factors that influencing the stability of these systems.

4. Experimental

4.1 Materials and methods

All solvents were dried over appropriate drying agents, degassed using a vacuum line and distilled under an Ar atmosphere. $[ReX(CO)_5]$ [28] and $[ReX(CO)_3(CH_3CN)_2]$ [29] were obtained by literature methods. The ligands $H_2(py)L^2$ and $H_2(Fe)L^2$ were obtained as reported previously [16, 17].

Elemental analyses were carried out on a Fisons EA-1108. Melting points (m.p.) were determined on a Gallenkamp MFB-595 and are uncorrected. Mass spectra were recorded on a VG Autospec Micromass spectrometer operating under FAB conditions (nitrobenzyl alcohol matrix). Infrared spectra were recorded from KBr pellets on a Bruker Vector 22FT. UV-Vis spectra were obtained on a CARY 100 (Varian) spectrophotometer. ^{1}H NMR spectra were obtained on a Bruker AMX 400 spectrometer from acetone-d_6 and DMSO-d_6 solutions.

Electrochemical studies were performed at 293 K in dry dichloromethane (concentration around 10^{-4} M) with tetrabutylammonium perchlorate as the supporting electrolyte using an Autolab Ecochemie potentiostat/galvanostat, an Ag/AgCl reference electrode,

a Pt wire as counter electrode and a 2 mm diameter disc of Pt or graphite as the working electrode.

4.2 X-ray data collection, structure determination and refinement

Crystallographic data collection and refinement parameters are listed in Table 3. All crystallographic measurements were performed on a Bruker Smart CCD apparatus at CACTI (University of Vigo) at r.t. (293(2) K) using graphite monochromated Mo-Kα radiation (λ = 0.71073 Å). The data were corrected for absorption effects using the program SADABS [30]. Structure analyses were carried out by direct methods [31]. Least-squares full-matrix refinements on F^2 were performed using the program SHELXL97. Atomic scattering factors and anomalous dispersion corrections for all atoms were taken from *International Tables for Crystallography* [32]. All non-hydrogen atoms were refined anisotropically. Hydrogen atoms were refined as riders. Graphics were obtained with PLATON [33] and MERCURY [34].

All crystals of compound **1b'** were non-merohedral twins and two components were identified using the CELL_NOW program [35]. SAINT-plus (version 6.29) was used for integration, TWINABS for the absorption correction [36, 37]} and the structure was solved using SHELXS97. A file including overlap of reflections was used for the final refinement using SHELXL97. However, some constraints were applied in the anisotropic parameters of some carbon atoms.

4.3 Data for ligands $H_2(py)L^2$ and $H_2(Fe)L^2$

$H_2(py)L^2$, ^{1}H NMR (DMSO-d_6, ppm): 11.80s (1) δ(O(2)-H); 11.50s (1) δ(N(1)-H); 8.60d (1) δ(C(13)-H); 8.10d (1) δ(C(10)-H); 8.00d (1) δ(C(7)-H); 7.90t (1) δ(C(11)-H); 7.40m (2) δ(C(12)-H, C(5)-H); 7.00m (2) δ(C(4)-H, C(6)-H); 2.50s (3) δ(C(14)-H). ^{13}C NMR (DMSO-d_6, ppm): δ = 161.80 C(1); δ = 156.24 C(9); δ = 154.77 C(8); δ = 152.08 C(3); δ = 148.56 C(13); δ = 136.56 C(11); δ = 133.44 C(5); δ = 130.75 C(7); δ = 124.03

C(12); δ = 120.28 C(10); δ = 119.72 C(6); δ = 117.82 C(2); δ = 116.79 C(4); δ = 11.67 C(14). UV-vis: λ in nm (ε × 10^{-3}; in L/mol.cm): MeOH as solvent 311(23200), 298(23800).

$H_2(Fe)L^2$,^{1}H NMR (DMSO-d_6, ppm): 12.10s (1) δ(O(2)-H); 11.60s (1) δ(N(1)-H); 8.30s (1) δ(C(8)-H); 7.90d (1) δ(C(7)-H); 7.40t (1) δ(C(5)-H); 6.95m (2) δ(C(4,6)-H); 4.70d (2) δ(C(10, 13)-H); 4.50d (2) δ(C(11,12)-H); 4.30s (5) δ(C(Cp)-H).

^{1}H NMR (acetone-d_6, ppm): 12.40s (1) δ(O(2)-H); 10.90s (1) δ(N(1)-H); 8.40s (1) δ(C(8)-H); 7.90d (1) δ(C(7)-H); 7.40t (1) δ(C(5)-H); 6.90m (2) δ(C(4,6)-H); 4.70d (2) δ(C(10,13)-H); 4.40d (2) δ(C(11,12)-H); 4.20s (5) δ(C(Cp)-H). UV-vis: λ in nm (ε × 10^{-3}; in L/mol.cm): $CHCl_3$ as solvent: 461(2116), 318(30391), 259(19848), 234(23515); MeOH as solvent: 458(1683), 315(26710), 266(15672). $E_{1/2}$ (V in CH_2Cl_2): 0.554.

*4.4 Synthesis of the complexes [ReX(CO)$_3$(H$_2$(py)L^2)] (**1a** X = Cl, **1b** X = Br)*

The rhenium complexes were synthesized by reaction of equimolar quantities of $H_2(py)L^2$ (33 mg, **1a**; 30 mg **1b**) with *fac*-[ReX(CO)$_3$(CH_3CN)$_2$] (50 mg, **1a**; 50 mg **1b**) in dry chloroform (10 mL) under reflux for 2 hours. The orange solid was filtered off and vacuum dried over $CaCl_2$. Single crystals of the compounds were obtained from an acetonitrile/acetone solution (for X = Cl and X = Br, respectively) on standing at room temperature for several days. The complexes were characterized by elemental analyses, FAB-MS, IR, UV-vis and ^{1}H NMR.

Data for **1a**

Yield: 63.6 mg (88.0%). M.p.: 270 ºC. Anal. found (%):C 36.70, H 2.59, N 7.62; $C_{17}H_{13}N_3O_5ClRe$ requires: C 36.40, H 2.34, N 7.49 Mass spectrum [*m*/*z* (%)]: 560.90(12.56) $[M]^+$, 525.93(35.22) $[M - Cl]^+$, 496.93(5.26) $[M - \{Cl,CO\}]^+$,

441.96(4.95) [M – {Cl,3CO}]$^{+}$. IR (ν/cm^{-1}): 3445m,br ν(OH)/ν(NH); 2027s, 1917vs, 1893vs ν(CO_{fac}); 1643m ν(C=O); 1605m, 1521m, 1480w ν(C=N) + ν(C=C). ^{1}H NMR (acetone-d_6, ppm): 11.30s (1) δ(O(2)-H); 11.55s (1) δ(N(1)-H); 9.10d (1) δ(C(13)-H); 8.50d (1) δ(C(10)-H); 8.40t (1) δ(C(11)-H); 8.10d (1) δ(C(7)-H); 7.90t (1) δ(C(12)-H); 7.55t (1) δ(C(5)-H); 7.10d (1) δ(C(4)-H); 7.00t (1) δ(C(6)-H); 2.75s (3) δ(C(14)-H). ^{1}H NMR (DMSO-d_6, ppm): 11.70s (1) δ(O(2)-H); 11.90s (1) δ(N(1)-H); 9.05d (1) δ(C(13)-H); 8.50d (1) δ(C(10)-H); 8.40t (1) δ(C(11)-H); 7.90d (1) δ(C(7)-H); 7.85t (1) δ(C(12)-H); 7.50t (1) δ(C(5)-H); 7.05m (2) δ(C(4)-H, C(6)-H); 2.60s (3) δ(C(14)-H). ^{13}C-NMR (DMSO-d_6, ppm): δ = 197.85, 196.46, 187.76 CO; δ = 176.87 C(1); δ = 162.27 C(3); δ= 157.16 C(8); δ= 153.24 C(13); δ= 153.22 C(9); δ= 140.24 C(11); δ= 134.07 C(5); δ= 129.87 C(7); δ= 129.54 C(12); δ= 128.83 C(10); δ= 119.49 C(6); δ= 116.91 C(2); δ= 116.25 C(4); δ= 16.88 C(14). UV-vis: λ in nm (ε × 10^{-3}; in L/mol.cm): $CHCl_3$ as solvent: 420(2613), 280(7802), 243(10905); MeOH as solvent: 384(3410), 291 nm (9041).

Data for **1b**

Yield: 53.1 mg (73.1%). M.p.: 269 ºC. Anal. found (%): C 33.68, H 2.15, N 6.94; $C_{17}H_{13}N_3O_5BrRe$ requires: C 33.73, H 2.16, N 6.94. Mass spectrum [*m*/*z* (%)]: 604.95(15.05) [M]$^{+}$, 576.96(8.79) [M – CO]$^{+}$, 526.03(32.31) [M – Br]$^{+}$, 497.03(3.51) [M – {CO,Br}]$^{+}$, 442.04(5.07) [M – {3CO, Br)]$^{+}$. IR (ν/cm^{-1}): 3449m,br ν(OH)/ν(NH); 2026s, 1919vs, 1892vs ν(CO_{fac}); 1643m ν(C=O); 1604m, 1516m, 1478w ν(C=N) + ν(C=C). ^{1}H NMR (acetone, ppm): 11.50s (1) δ(N(1)-H); 11.25s (1) δ(O(2)-H); 9.15d (1) δ(C(13)-H); 8.50d (1) δ(C(10)-H); 8.40t (1) δ(C(11)-H); 8.10d (1) δ(C(7)-H); 7.90t (1) δ(C(12)-H); 7.55t (1) (C(5)-H); 7.10d (1) δ(C(4)-H); 7.05t (1) δ(C(6)-H); 2.75s (3) δ(C(14)-H). ^{1}H NMR (DMSO-d_6, ppm): 11.85s (1) δ(N(1)-H); 11.80s (1) δ(O(2)-H); 9.05d (1) δ(C(13)-H); 8.50d (1) δ(C(10)-H); 8.40t (1) δ(C(11)-H); 7.90d (1) δ(C(7)-H);

7.85t (1) δ(C(12)-H); 7.50t (1) δ(C(5)-H); 7.05m (2) δ(C(4)-H, C(6)-H); 2.65s (3) δ(C(14)-H). ^{13}C NMR (DMSO-d_6, ppm): δ = 197.38, 195.93, 187.10 CO; δ = 176.76 C(1); δ = 162.12 C(3); δ = 157.00 C(8); δ = 153.42 C(9); δ= 153.42 C(13); δ= 153.24 C(9); δ = 140.16 C(11); δ = 134.07 C(5); δ = 130.00 C(7); δ = 129.45 C(12); δ = 128.92 C(10); δ = 119.53 C(6); δ = 116.88 C(2); δ = 116.33 C(4); δ = 16.89 C(14). UV-vis: λ in nm (ε × 10^{-3}; in L/mol.cm): $CHCl_3$ as solvent: 424(4789), 289(16445), 242(22705); MeOH as solvent: 381(6476), 285 (20417).

*4.5 Synthesis of the complexes [ReX(CO)$_3$(H$_2$(Fe)L^2)] (**2a** X = Cl, **2b** X = Br)*

The rhenium complexes were synthesized by reaction of equimolar quantities of $H_2(Fc)L^2$ with *fac*-bis(acetonitrile)bromotricarbonylrhenium(I) in dry chloroform (10 mL) under reflux for 2 hours. The red solids were collected by filtration and dried under vacuum over $CaCl_2$. Single crystals were obtained from a chloroform solution of [ReX(CO)$_3${H$_2$(Fc)L^2}] on standing at room temperature for several days. The complexes were characterized by elemental analyses, FAB-MS, IR, UV-vis and ^{1}H NMR.

Data for **2a**

Yield: 59.8 mg (70.9%). M.p.: 248ºC. Anal. found (%): C 38.39, H 2.39, N 4.17; $C_{21}H_{16}N_2O_5ClFeRe$ requires: C 38.57, H 2.47, N 4.28. Mass spectrum [m/z (%)]: 1272.47(4.67) [2M-Cl, H]$^+$, 653.82(17.93) [M]$^+$, 618.87(33.30) [M-Cl]$^+$, 347.94(39.54) [FcL^2]$^+$. IR (ν/cm^{-1}): 3444w,br ν(OH)/ν(NH); 2025s, 1938m,sh, 1909vs ν(CO_{fac}); 1608m ν(C=O); 1548m, 1491sh,w, 1457w ν(C=N) + ν(C=C). ^{1}H NMR (DMSO-d_6, ppm): 12.30s (1) δ(N(1)-H); 11.10s (1) δ(O(2)-H); 8.80s, 7.95s (1) δ(C(8)-H); 7.90d, 7.80d (1) δ(C(7)-H); 7.45t, 7.40t (1) δ(C(5)-H); 7.00m, 6.90m (2) δ(C(4,6)-H); 5.20s, 5.10d (2) δ(C(10,13)-H); 4.70m (2) δ(C(11,12)-H); 4.35s, 4.30s (5) δ(C(Cp)-H). ^{1}H

NMR (acetone-d_6, ppm): 12.50s (1) δ(N(1)-H); 11.00s (1) δ(O(2)-H); 9.00s, 8.40s (1) δ(C(8)-H); 8.20d, 8.10d (1) δ(C(7)-H); 7.65t, 7.60t (1) δ(C(5)-H); 7.25m, 7.15m (2) δ(C(4,6)-H); 5.25d, 5.15d (2) δ(C(10,13)-H); 4.90s, 4.85d (2) δ(C(11,12)-H); 4.50s, 4.40s (5) δ(C(Cp)-H). UV-vis: λ in nm (ε × 10^{-3}; in L/mol.cm): $CHCl_3$ as solvent: 497(4040), 297(24400), 259(27400), 235(24000); MeOH as solvent: 485(1320), 321(9950). $E_{1/2}$ (V in CH_2Cl_2): 0.730.

Data for **2b**

Yield: 66.5 mg (82.3%). M.p.: 257ºC. Anal. found (%): C 36.19, H 2.20, N 4.01; $C_{21}H_{16}N_2O_5BrFeRe$ requires: C 36.12, H 2.31, N 4.01. Mass spectrum [m/z (%)]: 697.86(6.91) $[M]^+$, 618.97(8.29) $[M\text{-}Br]^+$, 348.02(8.58) $[FcL^2]^+$. IR (ν/cm^{-1}): 3438vs,br ν(OH)/ν(NH); 2024s, 1909vs ν(CO_{fac}); 1607m ν(C=O); 1549m, 1521m, 1487w ν(C=N) + ν(C=C). ^{1}H NMR (DMSO-d_6, ppm): 12.30s (1) δ(N(1)-H); 11.10s (1) δ(O(2)-H); 8.80s, 7.95s (1) δ(C(8)-H); 8.80d, 7.90d (1) δ(C(7)-H); 7.45t, 7.35t (1) δ(C(5)-H); 7.90m, 6.95m (2) δ(C(4,6)-H); 5.20s, 5.10d (2) δ(C(10,13)-H); 4.70m (2) δ(C(11,12)-H); 4.35s, 4.30s (5) δ(C(Cp)-H). ^{1}H NMR (acetone-d_6, ppm): 12.30s (1) δ(N(1)-H); 11.10s (1) δ(O(2)-H); 9.00s, 8.40s (1) δ(C(8)-H); 8.20d, 8.10d (1) δ(C(7)-H); 7.70t, 7.60t (1) δ(C(5)-H); 7.25m, 7.20m, 7.15m (2) δ(C(4,6)-H); 5.25t, 5.15s (2) δ(C(10,13)-H); 4.90s, 4.85d (2) δ(C(11,12)-H); 4.50s, 4.45s (5) δ(C(Cp)-H). UV-vis: λ in nm (ε × 10^{-3}; in L/mol.cm): $CHCl_3$ as solvent: 502(1525), 299(9179), 262(10573), 227(7660); MeOH as solvent: 485(2250), 346(18100). $E_{1/2}$ (V in CH_2Cl_2): 0.720.

*4.6 Formation of the complex [[Re{H(py)L^2}(H$_2$O)(CO)$_3$] (**3**)*

Single crystals of [Re{H(py)L^2}(H_2O)$(CO)_3$] (orange) were obtained by diffusion of a solution of 13 mg (0.02 mmol) of [$ReBr(CO)_3${H_2(py)L^2}] in methanol (2 mL) over a solution of 5 mg (0.02 mmol) of copper(II) nitrate 2.5 hydrate in water (3 mL).

Mass spectrum [*m*/*z* (%)]: 525.83(19.60) [M – H_2O]$^+$, 496.85(11.64) [M – {H_2O,CO}]$^+$. IR (ν/cm^{-1}): 3446w,br ν(OH)/ν(NH); 2028s, 1926vs, 1893vs ν(CO_{fac}); 1597w, 1515w, 1485m (C=N) + ν(C=C).

Acknowledgements

Financial support from ERDF (EU), MEC (Spain) and Xunta de Galicia (Spain) (research projects CTQ2006-05642/BQU and PGIDIT06-PXIB314373PR) is gratefully acknowledged.

Appendix A. Supplementary data

Crystallographic data for the structural analysis have been deposited with the Cambridge Crystallographic Data Centre, CCDC numbers 727049 (**1a**), 727050 (**1b**), 727051 (**1b'**), 727052 (**2a**), 727053 (**2b**) and 727054 (**3**). These data can be obtained free of charge via www.ccdc.cam.ac.uk/conts/retrieving.html, or from the Cambridge Crystallographic Data Centre, 12 Union Road, Cambridge CB2 1EZ, UK; fax: +44 1223 336 033; or e-mail: deposit@ccdc.cam.ac.uk. Supplementary data associated with this article can be found, in the online version, at doi:10.1016/XXXXXX.

References

[1] W. Wang, B. Spingler, R. Alberto, Inorg. Chim. Acta, 355 (2003) 386-393.

[2] M. M. Saw, P. Kurz, N. Agorastos, T. S. A. Hor, F. X. Sundram, Y. K. Yan, R. Alberto, Inorg. Chim. Acta, 359 (2006) 4087-4094.

[3] (a) C. M. Alvarez, R. Garcia-Rodriguez, D. Miguel, Dalton Trans. (2007) 3546-3554. (b) (b) C. M. Alvarez, R. García-Rodríguez, D. Miguel, J. Organomet. Chem., 692 (2007) 5717-5726.

[4] R. S. Herrick, I. Wrona, N. McMicken, G. Jones, C. J. Ziegler, J. Shaw, J. Organomet. Chem., 689 (2004) 4848-48-55.

[5] V. W. Yam, K. M. Wong, V. W. Lee, K. K. Lo, K. Cheung., Organometallics, 14 (1995) 4034-4036.

[6] (a) A. J. Amoroso, M. P. Coogan, J. E. Dunne, V. Fernández-Moreira, J.B. Hess, A. J. Hayes, D. Lloyd, C. Millet, S. J. A. Pope, C. Williams, Chem. Commun., (2007) 3066-3068. (b) A. J. Amoroso, R. J. Arthur, M. P. Coogan, J. B. Court, V. Fernández-Moreira, A. J. Hayes, D. Lloyd, C. Millet, S. J. A. Pope, New J. Chem., 32 (2008) 1097-1102.

[7] M. A. Ali, R. N. Bose, Polyhedron, 3 (1984) 517-522.

[8] P. B. Sreeja, M. R. Prathapachandra Kurup, A. Kishore, C. Jasmin, Polyhedron, 23 (2004) 575-581.

[9] P. Barbazán, R. Carballo, B. Covelo, C. Lodeiro, J. C. Lima, E. M. Vázquez-López, Eur. J. Inorg. Chem., 2008 (2008) 2713-2720.

[10] J. Grewe, A. Hagenbach, B. Stromburg, R. Alberto, E. Vazquez-Lopez, U. Abram, Z. Anorg. Allg. Chem., 629 (2003) 303-311.

[11] B. K. Panda, S. Sengupta, A. Chakravorty, J. Organomet. Chem., 689 (2004) 1780-1787.

[12] S. Sengupta, B. K. Panda, Trans. Met. Chem., 30 (2005) 426-432.

[13] M. A. Ali, S. E. Livingstone, D. J. Phillips, Inorg. Chim. Acta, 7 (1973) 179-186.

[14] J. Fang, Z. Jin, Z. Li, W. Liu, App. Organomet. Chem., 17 (2003) 145-153.

[15] P. Barbazán, R. Carballo, U. Abram, G. Pereiras-Gabián, E. M. Vázquez-López, Polyhedron, 25 (2006/12/4) 3343-3348.

[16] P. Barbazán, R. Carballo, E. M. Vázquez-López, CrystEngComm, 9 (2007) 668-675.

[17] Z. Lu, W. Xiao, B. Kang, C. Su, J. Liu, J. Mol. Struct., 523 (2000/5/2) 133-141.

[18] R. Carballo, J. S. Casas, E. García-Martínez, G. Pereiras-Gabián, A. Sánchez, J. Sordo, E. M. Vázquez-López, J. C. Garcia-Monteagudo, U. Abram, J. Organomet. Chem., 656 (2002/8/15) 1-10.

[19] S. Parsons, G. A. Solan, R. E. P. Winpenny, C. Benelli, Angew. Chem. Int. Ed., 35 (1996) 1825-1828.

[20] K. A. Abboud, C. G. Ortiz, R. C. Palenik, G. J. Palenik, Acta Crystallogr. sect. C, 53 (1997) 1322-1323.

[21] R. Carballo, J. S. Casas, E. Garcia-Martinez, G. Pereiras-Gabian, A. Sanchez, J. Sordo, E. M. Vazquez-Lopez, Inorg. Chem., 42 (2003) 6395-6403.

[22] R. Carballo, A. Castiñeiras, S. García-Fontán, P. Losada-González, U. Abram, E. Vázquez-López, Polyhedron, 20 (2001) 2371-2383.

[23] B. R. Leeflang, J. F. G. Vliegenthart, L. M. J. Kroon-Batenburg, B. P. van Eijck, J. Kroon, Carbohydr. Res., 230 (1992/6/4) 41-61.

[24] D. T. McQuade, S. L. McKay, D. R. Powell, S. H. Gellman, J. Am. Chem. Soc., 119 (1997) 8528-8532.

[25] Y. S. Sohn, D. N. Hendrickson, H. Gray, J. Am. Chem. Soc., 93 (1971) 3603-3612.

[26] (a) A. Vogler, H. Kunkel, Coord. Chem. Rev., 200-202 (2000) 991-1008. (b) C. Garino, S. Ghiani, R. Gobetto, C. Nervi, L. Salassa, C. Croce, M. Milanesio, E.

Rosenberg, J. B. A. Ross, Eur. J. Inorg. Chem., (2006) 2885-2893 and references therein

[27] J. E. J. C. Graudo, C. A. L. Filgueiras, A. Marques-Netto, A. A. Batista, J. Braz, Chem. Soc., 11 (2000) 237-240.

[28] S. P. Schmidt, W. C. Trogler, F. Basolo, Inorg. Synth., 28 (1990) 160.

[29] M. F. Farona, K. F. Kraus, Inorg. Chem., 9 (1970) 1700-1704.

[30] G. M. Sheldrick, SADABS, University of Göttingen, Göttingen, RFA (1996).

[31] G. M. Sheldrick, *SHELX-97*, Program for the Solution and Refinement of Crystal Structures, v.2 University of Göttingen, Göttingen, RFA (1997).

[32] IUCr, International Tables for Crystallography., vol. C., A.J.C. Wilson (Ed.) Kluwer Academic Press, Dordrecht, The Netherlands (1992).

[33] A. L. Spek, *PLATON*, v. 21.08.03. University of Utrecht, The Netherlands (2002).

[34] I. J. Bruno, J. C. Cole, P. R. Edgington, M.K. Kessler, C.F. Macrae, P. McCabe, R. Taylor, Acta Crystallogr. sect. B 58 (2002) 389-397.

[35] G. M. Sheldrick, CELL_NOW, University of Göttingen, Göttingen, RFA (2008).

[36] G. M. Sheldrick, SAINT v. 6.22, 6.22, University of Göttingen, Göttingen, RFA (2001).

[37] G. M. Sheldrick, TWINABS, University of Göttingen, Göttingen, RFA (2008).

[38] W.C. Hamilton, Anonymous Statistic in Physical Science, The Ronald Press Company, New York, USA (1964),

Table 1. Selected interatomic bond distances (Å) and angles (º).

	1a	**1b**	**1b'** [a]	**2a.H_2O**	**2b.EtOH**	**3**
	X = Cl	X = Br		X = Cl	X = Br	X = H_2O
	Y= N(3)	Y= N(3)		Y= O(1)	Y= O(1)	Y= N(3)
Re–X	2.485(3)	2.6121(11)	2.612(1)	2.471(3)	2.6092(19)	2.164(5)
Re–Y	2.173(7)	2.160(6)	2.131(11)	2.128(7)	2.151(10)	2.174(5)
Re–N(2)	2.194(7)	2.177(6)	2.134(9)	2.156(8)	2.156(11)	2.185(5)
N(2)–C(8)	1.254(11)	1.324(9)	1.315(14)	1.296(11)	1.273(15)	1.299(7)
N(2)–N(1)	1.388(10)	1.383(7)	1.425(11)	1.397(10)	1.358(14)	1.405(7)
N(1)–C(1)	1.386(11)	1.369(9)	1.363(13)	1.357(12)	1.322(16)	1.312(8)
C(3)–O(2)	1.342(12)	1.338(11)	1.344(14)	1.354(11)	1.389(16)	1.372(8)
O(1)–C(1)	1.246(11)	1.229(10)	1.200(12)	1.242(12)	1.251(16)	1.281(7)
N(2)–Re–X	82.04(19)	82.49(18)	85.1(2)	83.2(2)	82.5(3)	79.69(18)
N(2)–Re–Y	73.9(3)	73.8(2)	72.9(4)	73.9(3)	74.7(4)	73.56(19)
X–Re–Y	85.2(2)	85.96(19)	82.2(2)	82.0(2)	85.7(3)	81.97(19)
C(8)–N(2)–N(1)	115.3(7)	116.1(6)	115.4(9)	116.2(10)	118.5(12)	116.5(5)
C(1)–N(1)–N(2)	122.3(7)	121.2(7)	120.3(8)	115.4(9)	119.4(12)	114.8(5)
N(2)–C(8)–C(9)	115.2(8)	115.8(7)	112.6(11)	133.6(11)	129.5(15)	115.4(5)
O(1)–C(1)–N(1)	118.1(8)	120.7(9)	120.5(11)	119.6(10)	119.8(14)	126.2(6)
O(1)–C(1)–C(2)	123.7(9)	122.2(9)	122.1(11)	121.3(10)	116.7(14)	119.2(6)
N(1)–C(1)–C(2)	118.2(9)	117.0(9)	117.3(11)	119.0(10)	123.4(14)	114.3(6)

[a] Data are average values estimated from the equations $\bar{x} = \left(\sum_{j=1}^{n} x_j / \sigma_j^2 \right) \sum_{j=1}^{n} 1/\sigma_j^2$ and $\sigma^2(\bar{x}) = 1 \Big/ \sum_{j=1}^{n} 1/\sigma_j^2$ [38]

Table 2. Selected intra- and intermolecular interactions (Å,º).[a]

D–H…A	d(D–H)	d(H…A)	d(D…A)	<(D–H…A)	reference
H₂(py)L²					[16]
N(1)–H(1)…O(2)	0.86	1.93	2.607(4)	134.6	
[H₃(py)L²]Cl.2H₂O					[20]
N(1)–H(1)…O(2)	0.86(2)	1.90(2)	2.615(2)	140(2)	
1a					this work
O(2)–H(2)...O(1)	0.82	1.85	2.582(10)	147.7	
N(1)–H(1)...Cl^{i}	0.86	2.54	3.381(8)	166.1	
C(11)–H(11)...O(22)^{ii}	0.93	2.47	3.237(13)	139.6	
C(14)–H(14A)...O(23)^{iii}	0.96	2.38	3.307(11)	162.4	
1b					this work
O(2)–H(2)...O(1)	0.82	1.84	2.569(9)	146.9	
N(1)–H(1)...Br^{i}	0.86	2.69	3.520(7)	162.2	
C(11)–H(11)...O(22)^{ii}	0.93	2.44	3.160(13)	133.7	
C(14)–H(14A)...O(23)^{iii}	0.96	2.40	3.316(11)	159.8	
1b'					this work
N(1A)–H(1A)...O(2A)	0.86	2.22	2.693(18)	114.3	
N(1A)–H(1A)...O(21B)^{iv}	0.86	2.56	3.341(19)	151.8	
O(2A)–H(2A)...O(1B)^{iv}	0.82	1.98	2.768(18)	162.0	
N(1B)–H(1B)...O(2B)	0.86	2.22	2.663(18)	112.3	
N(1B)–H(1B)...O(21A)	0.86	2.48	3.248(18)	149.6	
O(2B)–H(2B)...O(1A)	0.82	1.98	2.750(17)	155.8	
2a.H₂O					this work
N(1)–H(1)…O(2)	0.86	1.92	2.576(11)	131.4	
O(2)–H(2)…O(1W)	0.82	1.91	2.706(12)	163.3	
O(1)–H(1W)…Cl^{v}	0.955(10)	2.180(3)	3.131(11)	174.4(6)	
O(1W)–H(2W)…O(21)^{vi}	1.109(12)	2.160(10)	3.202(15)	155.4(6)	
O(1W)–H(2W)…O(22)^{vii}	1.109(12)	2.565(9)	3.197(15)	115.1(5)	
2b.EtOH					this work
N(1)-H(1)…O(2)	0.86	1.99	2.634(15)	131.2	
O(2)–H(2)…O(3)	0.82	1.81	2.586(15)	158.2	
O(3)–H(3)…Br^{viii}	0.82	2.56	3.308(14)	152.7	
O(3)–H(3)…O(22)^{ix}	0.82	2.68	3.154(18)	118.1	
3					this work
O(2)–H(2)...N(1)	0.82	1.80	2.522(7)	145.6	
O(1W)–H(2W)...O(1)	0.872(5)	2.158(4)	2.635(6)	113.9(3)	
O(1W)–H(1W)...O(1)^{x}	0.896(4)	1.794(4)	2.639(6)	156.1(3)	
[CuBr{H(py)L²}					[16]
O(2)–H(2)...N(1)	0.82	1.88	2.613(6)	147.6	
[Zn{H(py)L²}					[16]
O(2)–H(2)...N(1)	0.82	1.81	2.533(5)	147.0	

[a] Symmetry equivalent: i -x+2,-y,-z+2; ii x+½,-y+½,z-½; iii x+½,-y+½,z+½; iv x,y-1,z; v 1-x,2-y,1-z vi –x, 2-y, 1-z; vii x, 1+y, z; viii x+½,y+½,z; ix ½+x, -1/2+y, z; ix -x+1,-y+1,-z+2;

Table 3. Crystal data and data collection for the complexes.

	1a	**1b**	**1b'**	**2a.H_2O**	**2b.EtOH**	**3**
Empirical formula	$C_{17}H_{13}ClN_3O_5Re$		$C_{17}H_{13}BrN_3O_5Re$	$C_{21}H_{18}ClFe\ N_2O_6Re$	$C_{23}H_{22}BrFeN_2O_6Re$	$C_{17}H_{14}N_3O_6Re$
Formula weight	560.95		605.41	671.87	744.39	542.51
Crystal system	Monoclinic		Monoclinic	Triclinic	Monoclinic	Triclinic
Space group	P2(1)/n	P2(1)/n	P2(1)/c	P-1	Cc	P-1
a(Å)	13.3775(12)	13.269(2)	8.3703(14)	10.3249(13)	20.928(3)	8.2681(9)
b(Å)	9.4010(8)	9.6612(16)	11.7744(19)	10.4231(13)	6.1229(10)	9.4458(10)
c(Å)	14.7552(13)	14.769(3)	38.473(6)	10.6126(13)	21.074(3)	11.7340(12)
α (Å, º)				97.134(3)		102.688(2)
β (º)	98.057(2)	97.277(4)	92.659(4)	90.292(3)	115.358(3)	90.208(2)
γ (º)				103.565(3).		96.535(2)
Volume ($Å^3$)	1837.3(3)	1878.1(5)	3787.7(11)	1101.0(2)	2440.2(6)	887.84(16)
Z	4	4	8	2	4	2
Dc(Mg/m^3)	2.028	2.141	2.123	2.027	2.026	2.029
μ (mm^{-1})	6.793	8.631	8.559	6.314	7.229	6.884
θ range(º)	1.93–28.01	1.94–28.05	1.81–28.17	1.94–28.01°.	2.15–28.11°.	1.78–28.05
Index ranges	–17,17; –10,12; –19,16	–17,17; –10,12; –19,19	–10,10;–15,15;–29,50	–13,12; –13,12; –13,13	–27,22; –8,7; –24,27	–10,8; –11,12; –15,15
Independent reflections (Rint)	4252 (0.0794)	4249 (0.0801)	9065 (0.1690)	4593(0.0695)	4064(0.0882)	3910 (0.0525)
Goodness-of-fit on F^2	0.892	0.680	0.807	0.800	0.829	0.822
Final R1/wR2 [I>2σ(I)]	0.0419/0.0797	0.0432/0.0499	0.0718/0.0987	0.0518/0.0705	0.0504/0.0635	0.0426/0.0662
R1/wR2 (all data)	0.0877/0.1109	0.1362/0.0634	0.2232, 0.1254	0.1249/0.0903	0.1129/0.0765	0.0640/0.0709

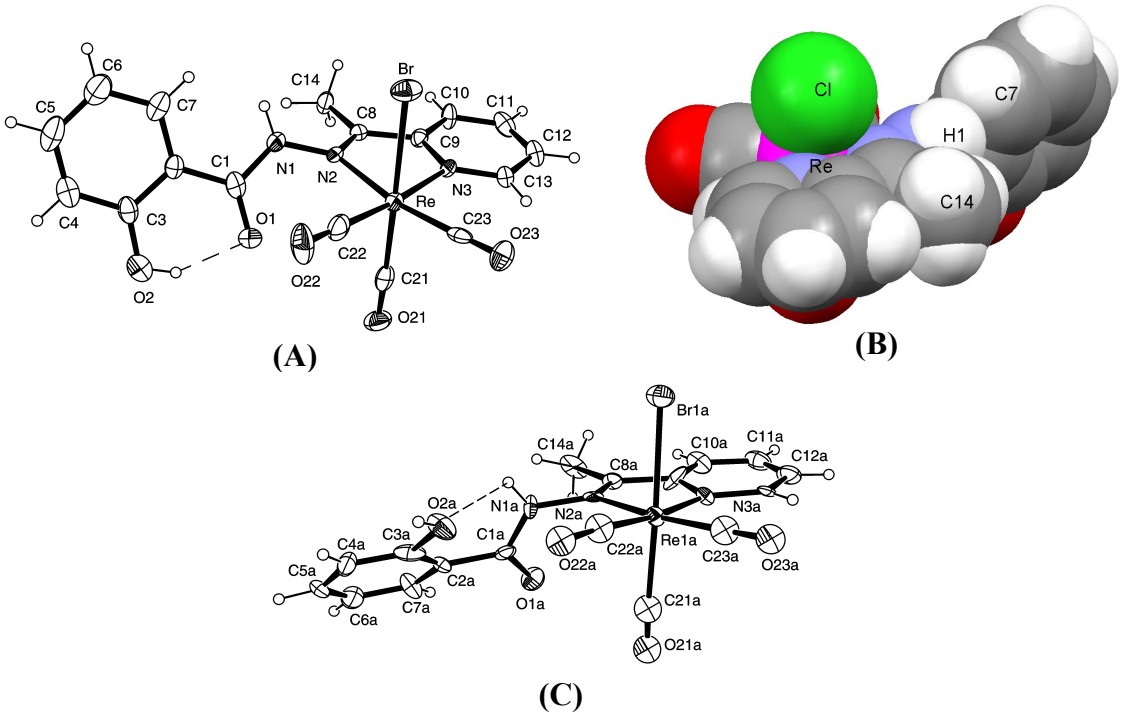

Figure 1. Molecular structures of the complexes **1b** (A), **1a** (B) and **1b'** (C).

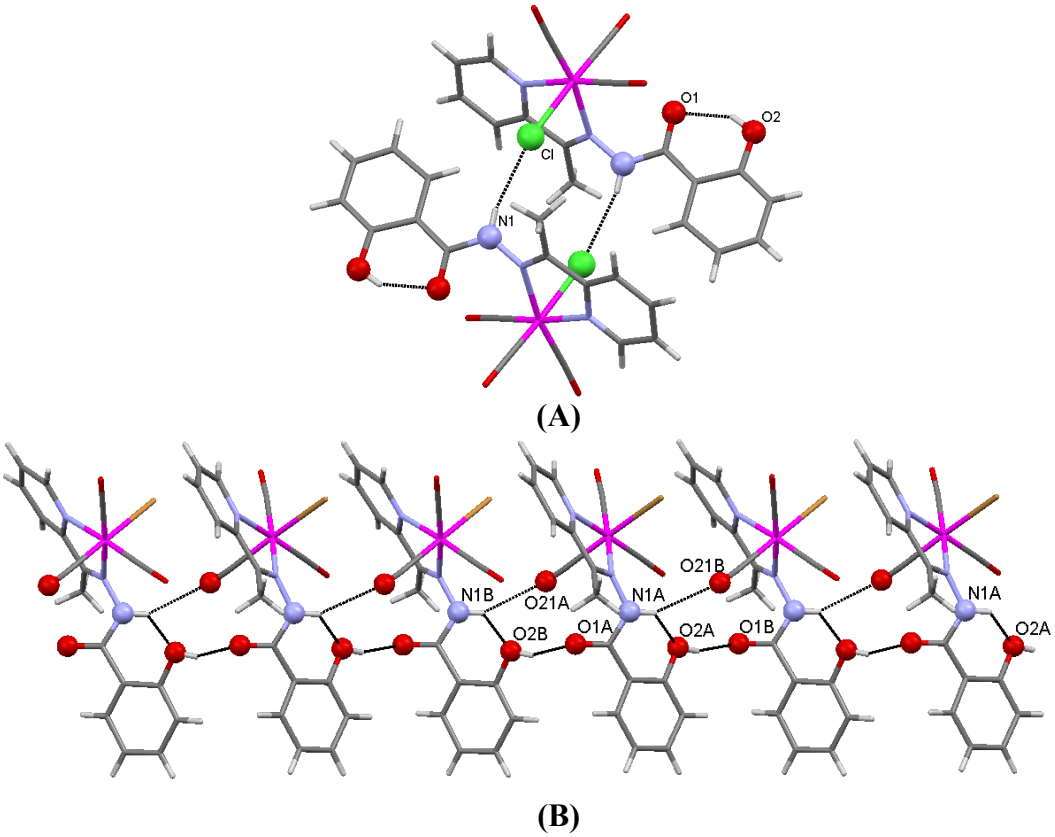

Figure 2. Molecular associations in **1a** (A) and **1b'** (B).

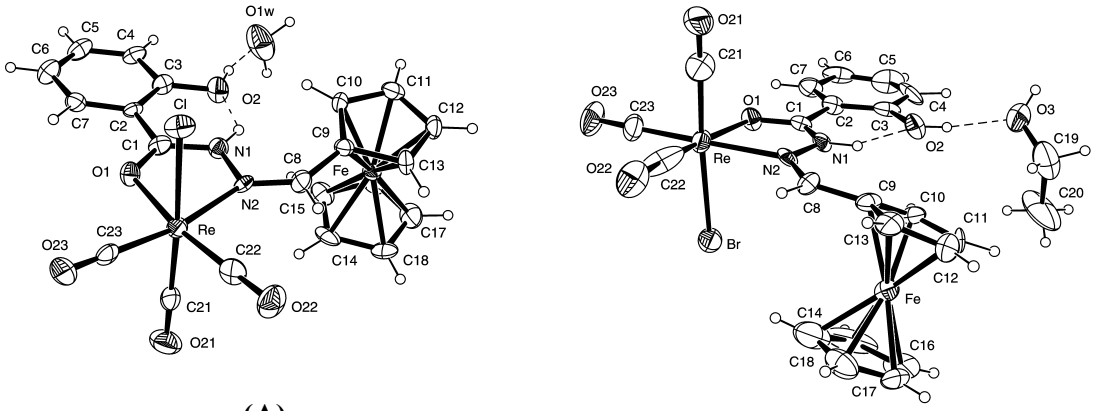

(A) **(B)**

Figure 3. Molecular structures of the complexes **2a** (A) and **2b**.

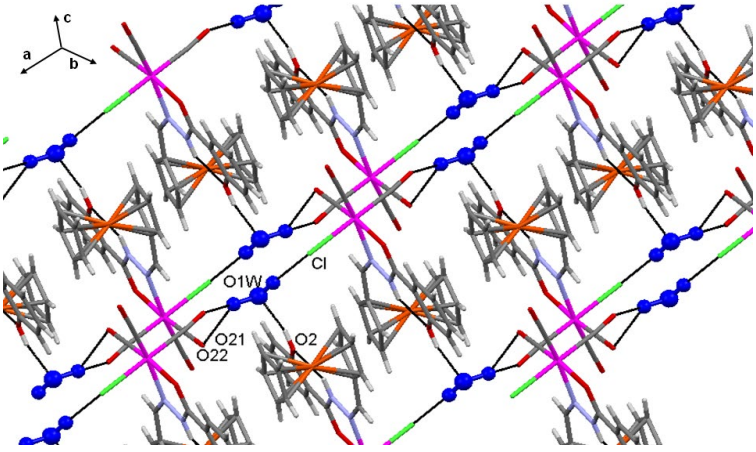

(A)

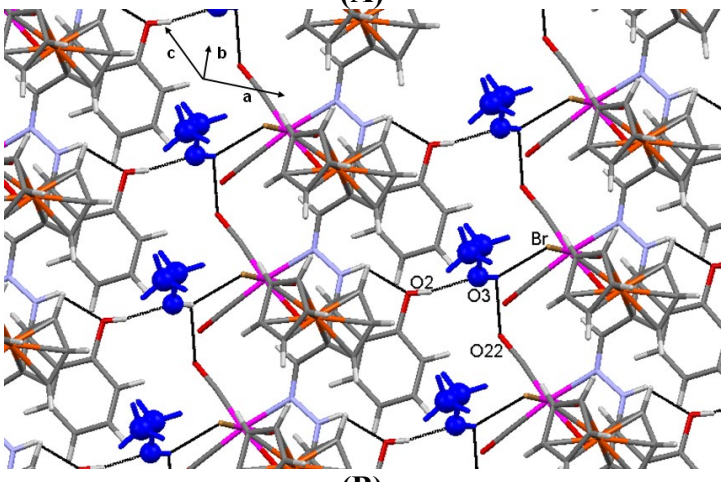

(B)

Figure 4. Molecular associations in **2a.H_2O** (A) and **2b.EtOH** (B).

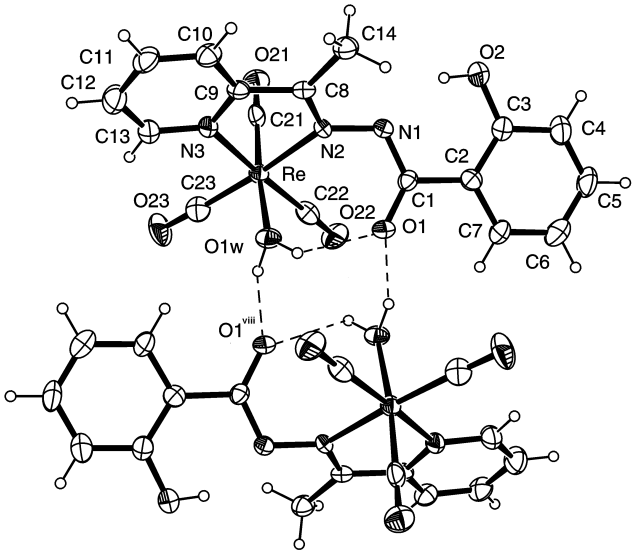

(F)

Figure 5. ORTEP showing the molecular association of **3** by hydrogen bonding.

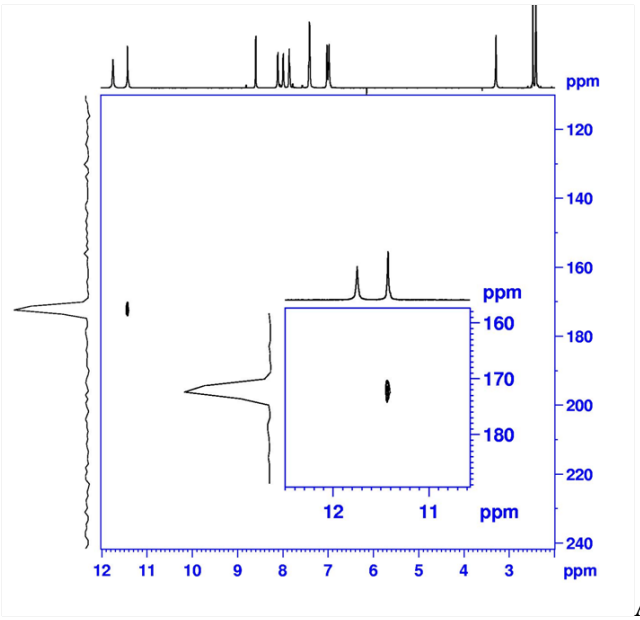

A)

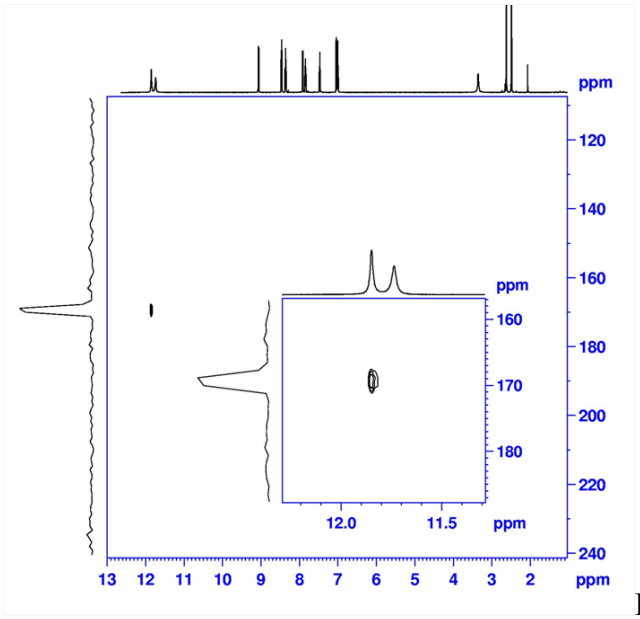

B)

Figure 6. ^{15}N-HSQC spectra for $H_2(py)L^2$ (**A**) and **1b** (**B**) in DMSO-d_6.